Class-E Silicon Carbide VHF Power Amplifier

Marc Franco, *Senior Member, IEEE*, and §Allen Katz, *Fellow*, *IEEE*

Linearizer Technology, Inc., 3 Nami Lane, Unit C-9, Hamilton, NJ, 08619, USA, §The College of New Jersey, Ewing, NJ, 08628, USA

Abstract **— Silicon carbide (SiC) Metal-Semiconductor Field Effects Transistors (MESFET) have been mostly employed in microwave and broadband radio frequency (RF) power amplifiers. This paper investigates an alternative use in high efficiency, class-E RF power amplifiers in the VHF range. Both simulation and experimental results are shown and demonstrate excellent agreement. A maximum drain dc to RF efficiency of 87% was predicted and 86.8 % achieved. The SiC MESFETs used in this project appear to offer significant advantages, particularly for space applications, over gallium arsenide (GaAs) transistors, which are inherently low voltage devices and more difficult to operate in class-E due to the high drain peak voltage occurring in this class of operation.**

Index Terms **— Power amplifiers, MESFET amplifiers, satellite communication, switching amplifiers.**

I. Introduction

Class-E amplifiers have been thoroughly described in the literature [1-4]. They provide very high dc to RF efficiency by operating the active device as a switch. One of the characteristics of class-E operation is the high peak voltage across the drain or collector of the active device. This voltage can be almost four times the voltage occurring in a class AB amplifier. High breakdown voltage devices are ideal candidates for these applications.

If an amplifier is intended to operate in space, radiation hardness becomes a concern. GaAs is the dominant semiconductor in space applications [5]. Unfortunately, GaAs devices have a low breakdown voltage, which makes them less convenient for operation in class-E. On the other hand, Lateral Double-diffused Metal Oxide Semiconductor (LDMOS) transistors have higher breakdown voltage, but generally cannot be used in high radiation environments.

The latest semiconductor technologies, gallium nitride (GaN) and SiC exhibit high breakdown voltages and robust radiation hardness desirable in space applications. While these devices have not yet been qualified for space, it is interesting to study their potential in class-E operation for certain military and weather satellites that make use of the VHF/UHF spectrum.

This paper describes the design, computer simulation and implementation of a 145 MHz class-E, high efficiency amplifier with a SiC MESFET. This amplifier will be part of the AMSAT-NA Eagle satellite's VHF/UHF software defined transponder that is currently under development [6].

The results of the amplifier nonlinear simulation agree very closely with the experimental results, confirming the accuracy of the device nonlinear model for VHF switching operation. The measured dc input to RF output efficiency is more than 86%, and it holds almost constant for a very wide range of drain voltages, even at constant input drive level. This excellent RF output voltage to drain dc voltage linearity enables the use of envelope elimination and restoration techniques that will be employed to reinstate the amplifier linearity required by the Eagle satellite.[7-8].

II. Amplifier Design And Implementation

The amplifier's design goal was an output power of 20 W at a frequency of 145 MHz, with no tunable parts, 100 KHz bandwidth, and harmonics and spurs at least 60 dB below the carrier. Cree's CRF24060 SiC MESFET was chosen as the active device for its high break down voltage, lack of internal matching, and availability of a nonlinear model. The amplifier's schematic diagram is shown in Fig. 1. Although not shown in the figures, all microstriplines were included in the simulation for improved accuracy.

The output waveform shaping network was designed according to the equations provided in [1] for a Q of 2.27. A maximum drain voltage of 30 V was used in order to avoid exceeding the device's maximum drain voltage. The output load impedance of approximately 18 ohms was matched to 50 ohms with an L network that shares the inductor with the waveform shaping network. Finally, a low pass filter section for improved spectral purity was utilized.

The input of the active device was matched to 50 ohms by means of a high pass filter network, in order to prevent the attenuation of the high frequency components of the drive signal.

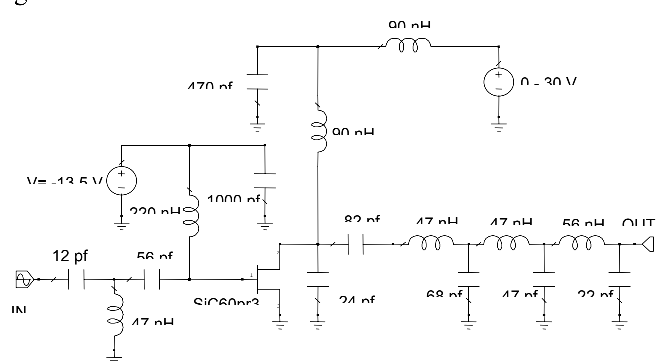

Fig. 1. Simplified SiC class-E VHF amplifier schematic.

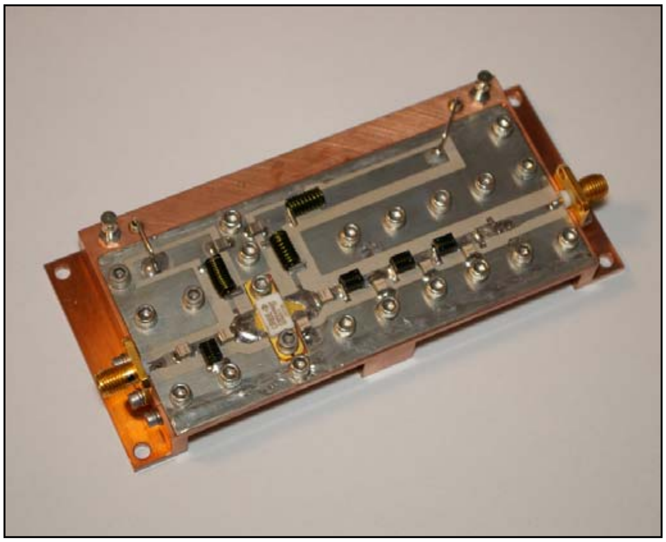

Fig. 2. High efficiency SiC MESFET class-E VHF amplifier.

Since it was desired to provide linear amplification by restoring the input signal's envelope with drain amplitude modulation, the drain bias network was built with a low pass filter that allows drain amplitude modulation frequencies of up to a few MHz to pass through it with minimum attenuation, while at the same time providing acceptable isolation at the carrier frequency and its harmonics.

The amplifier component values were optimized with AWR Microwave Office nonlinear simulator. Every effort was made to utilize standard value components, and to avoid the use of trimmer capacitors or adjustable inductors.

The amplifier prototype, shown in Fig. 2, was implemented on a Rogers 6002 30 mil substrate for its excellent outgassing and thermal characteristics, which make it suitable for space applications. ATC 700B standard value ceramic capacitors were used for the matching and biasing networks. Coilcraft air spring inductors with 2% tolerance were utilized throughout the design; however, the flight unit will employ inductors with no plastic coating.

III. SIMULATION AND EXPERIMENTAL RESULTS

The amplifier's performance was simulated with AWR Microwave Office and Cree's SiC MESFET nonlinear model. Measurements were later performed with the amplifier shown in Fig. 2. The simulation and experimental results were almost identical, to the extent that not a single component value change was necessary in order to obtain the simulated performance.

A. Performance as a function of drain voltage

Fig. 3 shows the amplifier RF output power as a function of drain voltage. This test was carried out with a constant input power level of 27 dBm, achieving the desired output power of 20 W and a power gain of 16 dB. Only the fundamental component of the output was considered in this measurement since the amplifier has a built-in low pass filter and all harmonics and spurs were at least 60 dB below the fundamental.

The drain efficiency as a function of drain voltage is shown in Figure 4. This efficiency was again measured at a constant input power level of 27 dBm. The efficiency was approximately constant and around 86% from a drain voltage of 2 V up to the maximum drain voltage of 30 V. Figure 5 shows the power added efficiency (PAE) of the amplifier for a constant drive level of 27 dBm.

The RF peak output voltage as a function of drain voltage is shown in Fig. 6, and illustrates the amplifier's excellent drain voltage to RF voltage linearity.

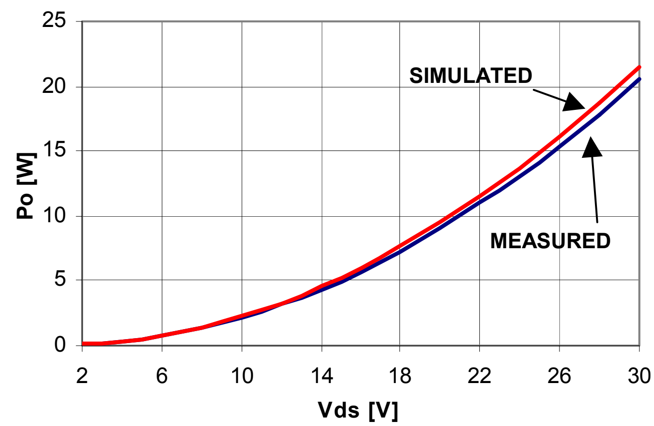

Fig. 3. RF output power as a function of drain voltage.

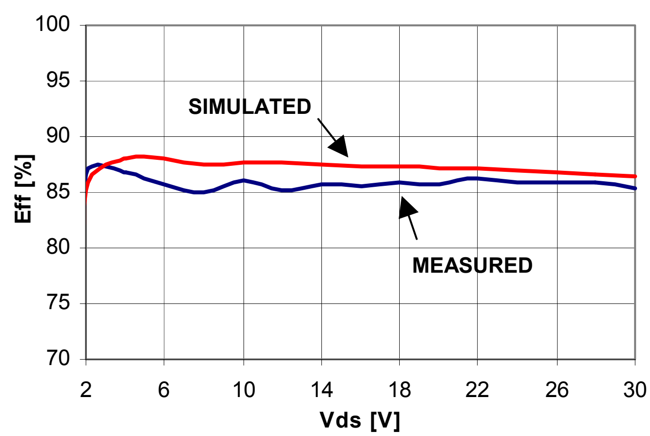

Fig. 4. Drain efficiency as a function of drain voltage.

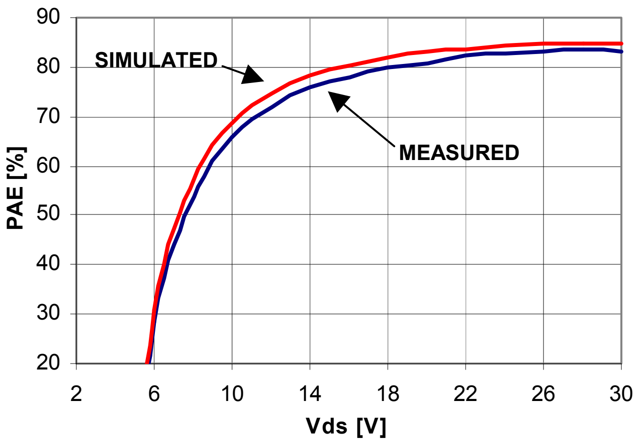

Fig. 5. Power added efficiency as a function of drain voltage.

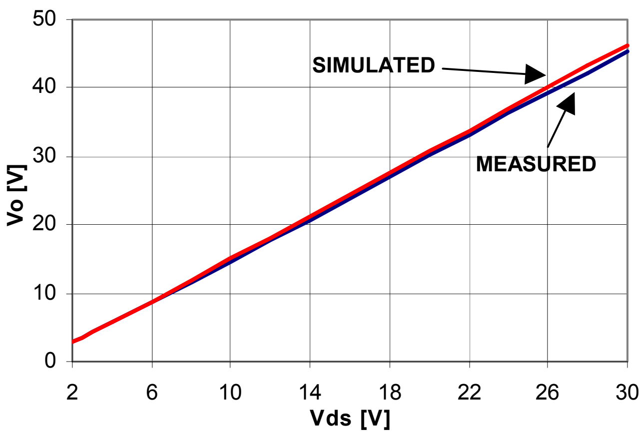

Fig. 6. RF peak output voltage as a function of drain voltage.

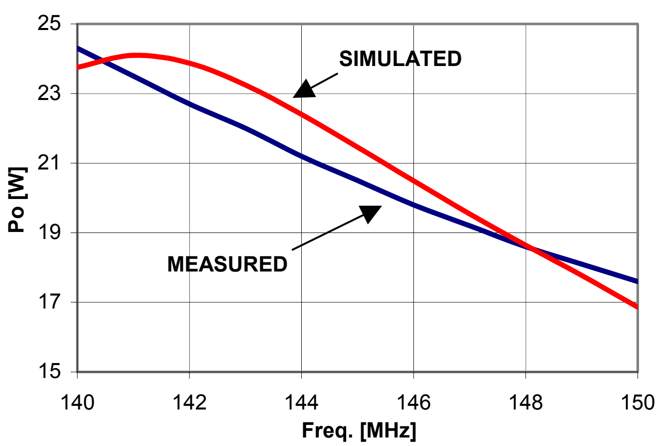

Fig. 7. RF Output power as a function of frequency.

B. Performance as a function of frequency

The amplifier design bandwidth goal was 100 KHz. However, it was evaluated over a 10 MHz bandwidth in order to determine its potential for wider bandwidth systems.

Fig. 7 shows the output power as a function of frequency. The simulated and experimental results are very similar. Both indicate a tendency to higher output power at lower frequencies. However, the efficiency of the amplifier degrades by a 2 to 3 % at the higher power levels, making the center frequency of 145 MHz the best compromise.

Fig. 8 shows the measured output spectrum of the amplifier. The simulation predictions and measured level for the second harmonic were identical at 58 dB below the fundamental. However, the measured third harmonic was approximately 20 dB higher due to coupling effects not taken into account during the simulation.

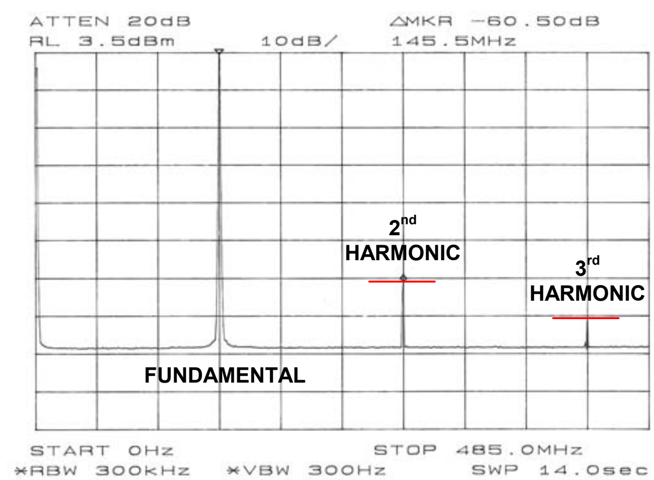

Fig. 8. Measured output spectrum.

C. Tuning the amplifier for higher efficiency

Simulations were run in order to optimize the drain efficiency. It was found that for lower output powers, the efficiency was slightly higher. For an output power of 15 W, a drain efficiency of almost 90 % was achieved.

Since the on-resistance of the active device will ultimately limit the maximum achievable drain efficiency, lowering the output power for a given drain voltage proportionally decreases the drain current [9]. As a result, the voltage drop across the device on-resistance also decreases.

The device on-resistance was measured and calculated from the nonlinear model to be in the order of 0.6 ohm.

IV. Future Work

The class-E, high-efficiency RF power amplifier described in this paper is intended to be used in a software-defined linear transponder. Since very high linearity is desired in this application, an envelope elimination and restoration system will be implemented in order to linearize the amplifier.

V. Conclusion

A high-efficiency class-E amplifier was designed, simulated and demonstrated practically. The simulation and the experimental results agreed so closely, that no component values changes were necessary.

A silicon carbide MESFET was used as the active device. This semiconductor technology has not been previously reported to be successful in producing very high efficiency VHF amplifiers. Since SiC devices operate from higher voltages than GaAs devices, they can be advantageously used in class-E designs. Given the possibility of SiC devices becoming space qualified, they could constitute the semiconductor of choice for these applications.

The most significant simulation and experimental results are summarized in Table I. A maximum drain dc to RF efficiency of 86.8 % was achieved. All measurements were done at a constant input power level of 27 dBm. The maximum power added efficiency for this drive level was measured at 83.5 %. A 20.5 W output power level was reached at a 30 V drain voltage.

Acknowledgement

The authors wish to acknowledge Cree, Inc., Durham, NC, for providing the MESFET nonlinear model and sample devices, and Dr. Allan Guida and Dr. Richard Campbell for reviewing the manuscript.

TABLE I
SiC Class-E Amplifier - Summary of Simulated and Experimental Results

Parameter	Simulated	Measured
Maximum Output Power	21.5 W	20.5 W
Nominal Input Power	27 dBm	27 dBm
Maximum Drain Efficiency	88 %	86.8 %
Maximum Power Added Efficiency	84.8 %	83.5 %
Maximum spurs and harmonics	-58 dBc	-58 dBc

References

[1] N. O. Sokal and A. D. Sokal, “Class E – A New Class of High-Efficiency Tuned Single-Ended Switching Power Amplifiers,” *IEEE Journal of Solid-State Circuits*, vol. SC-10, no. 3, pp. 168-176, June 1975

[2] F. H. Raab, “Class-E, Class-C, and Class-F Power Amplifiers Based Upon a Finite Number of Harmonics,” *IEEE Trans. Microwave Theory & Tech.,* vol. 49, no. 8, pp. 1462-1468, August 2001.

[3] H. L. Krauss, C. W. Bostian, and F. H. Raab, *Solid State Radio Engineering*, New York: J. Wiley & Sons, 1980.

[4] W. H. Cantrell, “Tuning analysis for the high-*Q* class-E power amplifier,” *IEEE Trans. Microwave Theory & Tech.,* vol. 48, no. 12, pp. 2397-2402, December 2000.

[5] T. R. Weatherford and W. T. Anderson Jr., “Historical perspective on radiation effects in III-V devices,” *IEEE Transactions on Nuclear Science*, vol. 50, no. 3, June 2003.

[6] R. Hambly, “Eagle Digital Design Meeting”, *The AMSAT Journal*, vol. 29, no. 4, pp. 3-4, July/August 2006.

[7] L. R. Kahn, “Single Sideband transmission by Envelope Elimination and Restoration,” *Proc. IRE,* vol. 40, no. 7, pp. 803-806, July 1952.

[8] D. Rudolph, et al, “Kahn EER Technique with Single-Carrier Digital Modulations,” *IEEE Trans. Microwave Theory & Tech.,* vol. 51, no. 2, pp. 548-552, August 2001.

[9] R. Negra, W. Bachtold, “Lumped-Element Load-Network Design for Class-E Power Amplifiers,” *IEEE Trans. Microwave Theory & Tech.,* vol. 54, no. 6, pp. 2684-2690, June 2006.